ENERGY DEPENDENT RANGE BIASES FOR SINGLE–PHOTON–DETECTION SYSTEMS.

GRAHAM APPLEBY AND PHILIP GIBBS

Royal Greenwich Observatory, Cambridge and Herstmonceux, UK

1. Introduction.

We have carried out experimental ranging to both target board and satellites in order to quantify potential energy–dependent range bias in the observations. We obtain biases relative to single–photon ranging of up to 40 mm for return levels of around 1000 photons. We use our models of the system response and of satellite signatures to compute the expected biases, and compare with the observations. We confirm the presence of an energy–dependent bias intrinsic to the SPAD detector.

2. High Energy Experiments.

2. 1. TARGET–BOARD RANGING.

We compute the return rate from ranging sessions by counting the number of laser shots in a given time interval, say 15 seconds. For each of these shots we check whether a noise event is detected, each of which reduces by one the effective number of laser shots. Given the number of true returns within the interval, we compute the true return rate as a percentage of the corrected number of laser shots. This information is displayed to the observer in near realtime. For a detector with quantum efficiency q, where $(0 < q < 1)$, we can relate the return rate to the number n of photons reaching the detector from

$$rate = (1 - e^{-(qn)}) \times 100$$

For the SPAD we have qe=0.2. For standard calibration ranging this rate is maintained at about 10-15% by attenuation of the outgoing laser beam, and by selection from a set of ND filters in the receive path, so that $n \leq 1$. For the duration of the ranging experiments the outgoing beam was attenuated such that the highest value ND filter was required to maintain single-photon returns. A series of calibration ranges was performed at different receive levels by selection of different ND filters, such that some 12 return levels of between 1 and 1000 photons were obtained. We note that for n above about 15, the observed return rate is close to 100%, so for rates $\geq$ 100%, n is estimated from the known relationships between the densities of the filters. The observations at each return level were used to form iterated mean

2.5

calibration values and single–shot rms precision, with rejection of outliers at 3 × rms. The calibration and precision values are shown in Figure 1 as functions of return energy level, where we plot data both from the full dynamic range of the experiment as a function of $Log(n)$, and as a function of return rate (0–100 %). For this latter sub-set it is seen that the calibration value changes by about 15 mm. The range precision changes little, with mean value about 9 mm, but with a temporary *decrease* to 13 mm at around 20%. This precision decrease has been noted consistently in the Herstmonceux data, and is also seen by Prochazka (1993) in laboratory tests of the SPAD. For the results over the full range of the experiment, we see that the calibration value changes by some 40 mm, and the single-shot precision increases to about 6mm.

2. 2. MODEL OF TARGET-BOARD RESULTS.

We have developed a model of the system response which closely represents the observed distribution of single–photon returns from the target board (Appleby, 1995, these proceedings). We now simulate our energy–dependent experiments by sampling from the model a given mean number n photons reaching the detector, as described in detail in Appleby (1993). We sample from the distribution a large number of times (> 500), finally forming from the simulated data the peak, the 3 × rms iterated mean, and the Leading–Edge, Half–Maximum (LEHM), using the procedure developed by Sinclair (1993).

We have plotted as the dotted line over the full zero-1000 photon return level these mean values, and also present in Table 1 the numerical values of change of calibration value as represented by the peak, the mean and LEHM. We see from comparing our model to the observations that the model under-estimates by some 25 mm the total change in calibration value, and that the model tends to 'flatten out' at high return level as 'photons' are sampled from close to the leading edge of the modelled distribution.

We now add to these model values an estimate of an energy-dependent timewalk intrinsic to the SPAD system by using the measurements of Prochazka (1993) over a dynamic range of between zero and 200 photons. The results of this complete model are shown as the full lines in Figure 1, where we plot the mean values.

We now find agreement between the observations and the model at most return levels, where the model agrees with the observed change at the 1-2 mm level, showing that the laser contributes only about 50% of the observed effect over the range of zero to 1000 photons. However, at the higher levels of return, the model over-estimates the total effect by some 4 mm, and does not fully model the observed increase in single-shot precision. Clearly, we have over-estimated the timewalk intrinsic to the SPAD, or our estimate of the laser pulse–width is too large. However, on the assumption that we have correctly estimated the pulse–width, the results from this experiment suggest that the timewalk for our device is some 15 mm, or 100 ps, over a dynamic range of from zero to 200 photons.

2. 3. SATELLITE RANGING.

We might expect that the bias effects measured from target-board ranging would also be present during satellite ranging if we depart from the single-photon regime. For this experiment, we observed nighttime passes of the satellites ERS-1, Meteor-3, Starlette, Stella, Lageos and Topex/Poseidon. At intervals throughout each pass the return levels were changed rapidly between single and multi–photons by removing or inserting ND filters in the receive path. For each pass the single–photon observations were reduced in the standard way, and then the deduced smoothing functions removed from the multi–photon data. The post solution residuals for all six passes are shown in Figure 2, where 'steps' of between 10 and 40 mm are clearly evident. For each pass we have computed separately the peak values and precision of the single and multi–photon sections of the data, and these values are displayed in Figure 3. From the known densities of the ND filters required to maintain single–photon levels we have estimated the numbers n of photons reaching the detector during the high-level return phases.

2. 4. MODELLING OF SATELLITE RESULTS.

Analogous to our model of the target-board results, we have modelled the satellite 'steps' as a function of the numbers of photons reaching the detector. We used for Lageos the model derived in Appleby (1995, these proceedings) from the satellite impulse function of Neubert (1995). We digitized the responses for ERS-1 from the curves derived by Degnan (1993), estimated the Starlette and Stella responses from the same source, and used the Topex/Poseidon responses of Varghese (Varghese and Pearlman, 1992). We do not currently have a model of the response of the small Meteor–3 LRA. We convolved these responses with our system response as characterized by the temporal distribution of the target-board ranges, and sampled from the resulting probability distributions in order to predict the range 'steps'. To these 'step' values we then added the intrinsic bias due to the SPAD, as deduced in the target board experiments. The results of the pass–averaged high and low–energy residual peak values and precision estimates, and the observed and predicted steps are shown in Table 2, along with the mean numbers of photons Np. In most cases as expected the multi-photon data has the greater single-shot precision, and the predicted 'steps' are in reasonable agreement with the observations, given the quoted observational precision values.

2. 5. LAGEOS COM VALUES

We have used the above simulations to model the changes to the Lageos CoM correction appropriate to a range of return energy levels. The results are given in Table 1 following the equivalent calibration values, and again are quoted as peak, 3 × rms iterated mean and LEHM. The CoM values have been calculated from the Lageos response model, followed by *subtraction* of the equivalent change of calibration value at each particular return energy level. We note that this correction

implies that calibration and satellite ranging are always carried out at the same energy level; if this is not true, much larger corrections to CoM may be appropriate, depending on the differences in energy. We see that the CoM correction for LEHM processing is little affected by return energy level, as may be anticipated from that statistic's lack of influence from the tail of the distribution. The peak value of CoM is less affected than that of the mean.

3. Conclusion.

We have shown that for our SPAD–based system, departure from the regime of single–photon return levels will result in range bias. We have experimentally examined the degree of bias as a function of return level, over a range of energy from single to 1000 photons. Simple statistical modelling of the system adequately explains the observational results, and implies that finite pulse-length accounts for about half the bias, and a plausible degree of energy-dependent time-walk within the SPAD system accounts for the remainder. For satellite ranging we find similar energy-dependent biases, which again are adequately explained by our models which include the effect of each satellite's response function. We conclude that if significant departures from single photons do occur during satellite passes, then the data should either be corrected using a measurement of the calibration dependence of the system on receive energy level, or sufficient information on the actual receive energy be included with each raw data point or normal point in order that analysts be able to compute appropriate CoM corrections. We finally note that provided calibration ranging and satellite ranging continue to be carried out at a strictly single–photon level, our normal practice, then range bias is minimal, at the expense of some loss of single–shot precision.

References

Appleby, G.M, 1993. Satellite Signatures in SLR Observations, NASA Conf. Proc 3214, Eighth International Workshop on Laser Ranging Instrumentation, Anapolis, MD, May 1992.

Degnan, J.J, 1993. Millimeter Accuracy Satellite Laser Ranging : A Review. Contributions of Space Geodesy to Geodynamics : Technology, Geodynamics 25, AGU.

Neubert, R. : 1995, "An Analytical Model of Satellite Signature Effects", In press in *Proc. Ninth Int. Workshop on Laser Ranging Instrumentation*, Canberra.

Prochazka, I, 1993. Single Photon Avalanche Diode Detector Package; Upgrade kit for RGO, July 1993.

Sinclair, A.T. : 1993, "SLR Data Screening; Location of Peak of Data Distribution". In *Proc. Eighth Int. Workshop on Laser Ranging Instrumentation*, Annapolis, MD

Varghese, T and M. Pearlman, 1992 September. SPAD Operations on the Topex/Poseidon Retroreflector Array, Private Communication.

Figure 1.

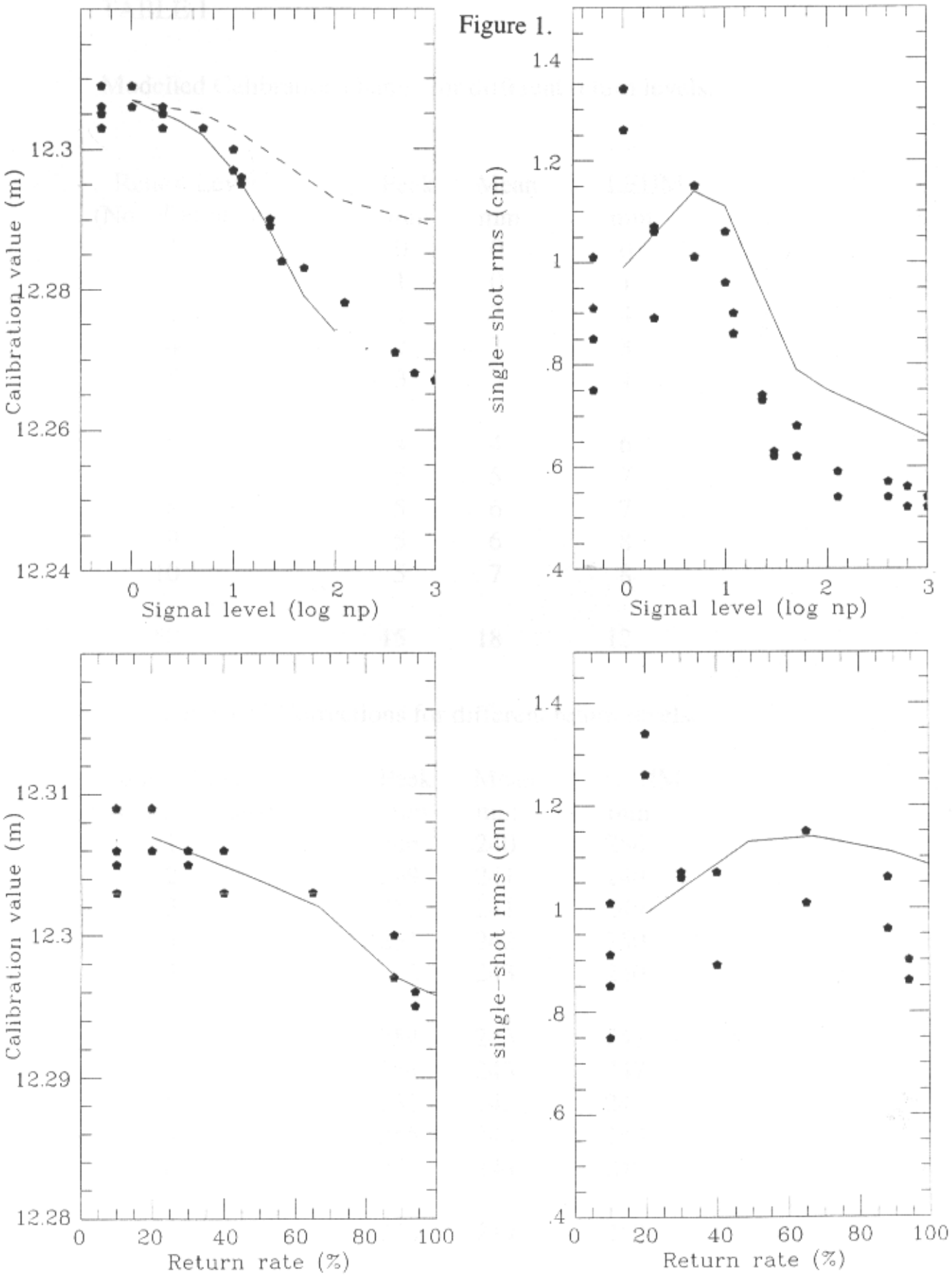
Calibration value (m)
12.3
12.28
12.26
12.24
0
1
2
3
Signal level (log np)
single-shot rms (cm)
1.4
1.2
1
.8
.6
.4
0
1
2
3
Signal level (log np)
Calibration value (m)
12.31
12.3
12.29
12.28
0
20
40
60
80
100
Return rate (%)
single-shot rms (cm)
1.4
1.2
1
.8
.6
.4
0
20
40
60
80
100
Return rate (%)

TABLE 1.

Modelled Calibration change for different return levels.

Return Level (No. of Photons)	Peak mm	Mean mm	LEHM mm
1	0	0	0
2	1	0	1
3	1	2	4
4	2	3	3
5	3	3	4
6	4	4	6
7	5	5	7
8	5	6	7
9	5	6	8
10	5	7	8
50	15	18	12

LAGEOS CoM Corrections for different return levels.

Return Level (No. of Photons)	Peak mm	Mean mm	LEHM mm
1	246	240	250
2	249	241	249
3	252	241	249
4	251	242	250
5	252	243	250
6	254	243	248
7	254	243	247
8	255	242	248
9	255	243	248
10	257	244	248
50	250	249	250

Figure 2.

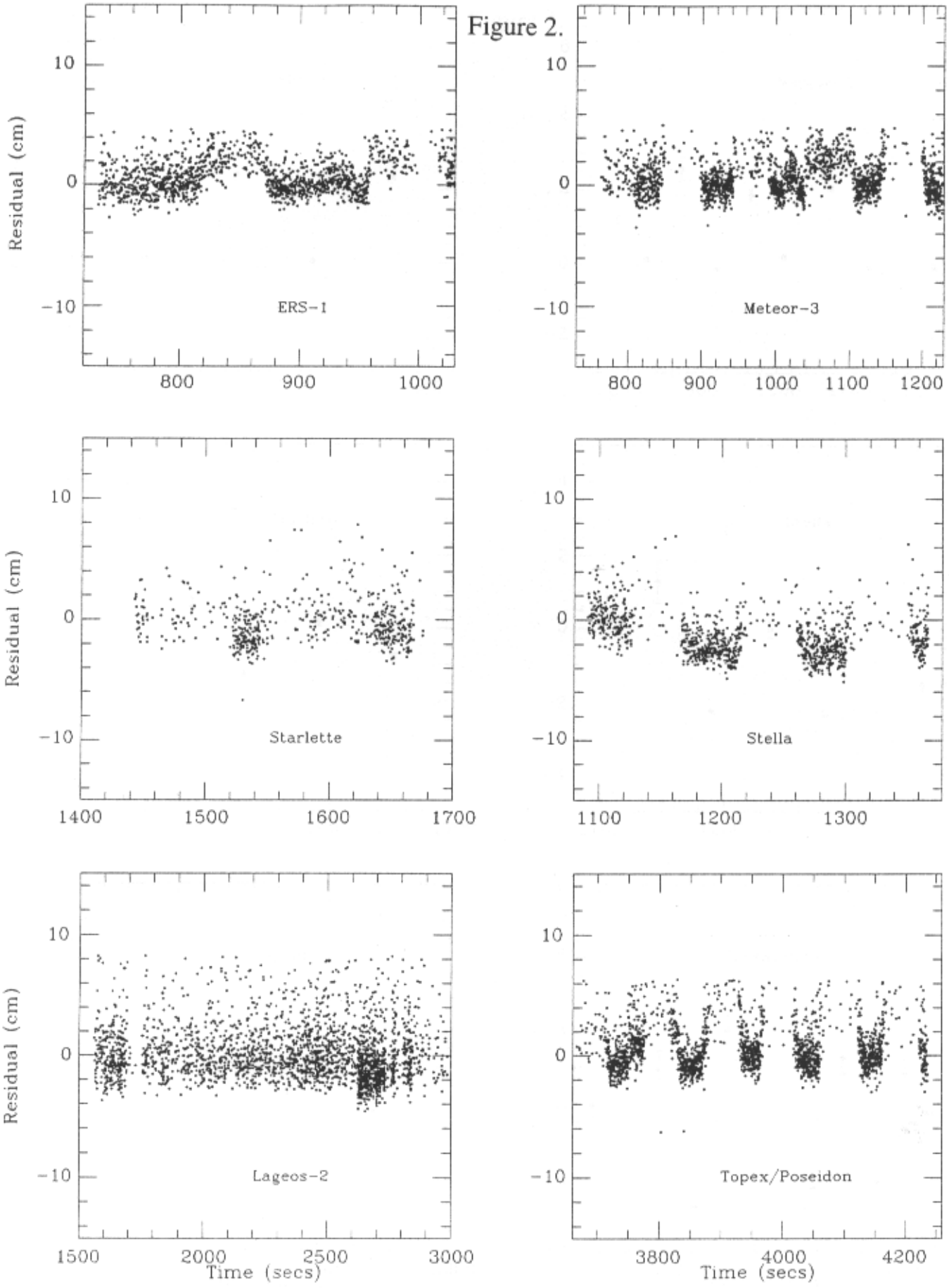
Residual (cm)
10
0
−10
ERS-1
800
900
1000
Meteor-3
1100
1200
Starlette
1400
1500
1600
1700
Stella
1300
Lageos-2
2000
2500
3000
Time (secs)
Topex/Poseidon
3800
4000
4200

Figure 3.

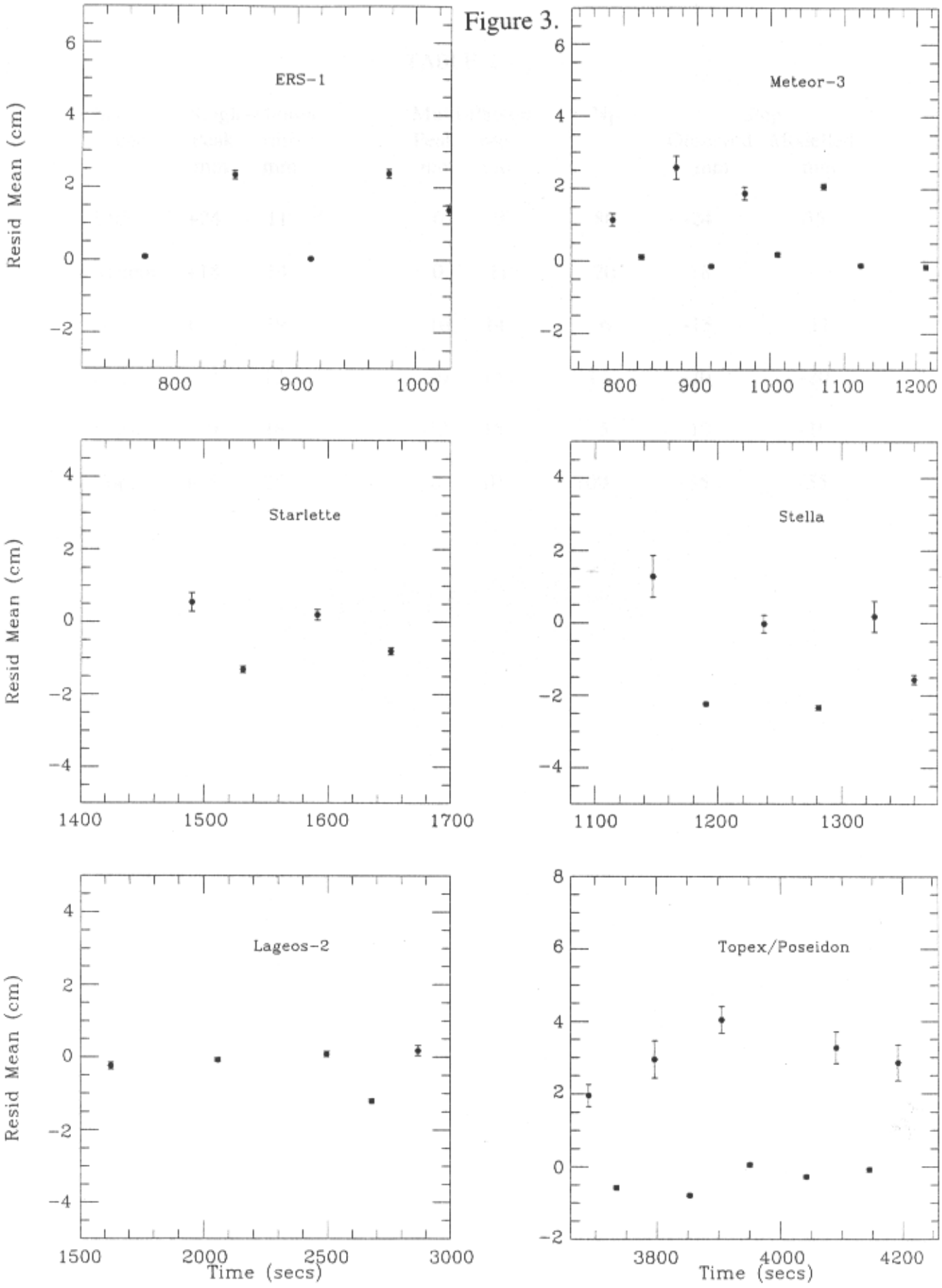
ERS-1
Meteor-3
Starlette
Stella
Lageos-2
Topex/Poseidon
Resid Mean (cm)
Time (secs)

TABLE 2

Sat Name	Single-Photon Peak mm	Single-Photon rms mm	Multi-Photon Peak mm	Multi-Photon rms mm	Np	Step Observed mm	Step Modelled mm
ERS-1	+24	11	0	9	80	-24	-35
Meteor	+18	14	0	11	20	-18	-
Star	+ 5	19	-10	14	6	-15	-11
Stell	0	12	-20	13	12	-20	-20
Lag-2	0	16	-12	15	5	-12	-10
Topex	+35	25	0	10	100	-35	-55